Clays and Clay Minerals, Vol. 56, No. 6, 660–676, 2008.

SEDIMENTOLOGICAL AND MINERALOGICAL INVESTIGATION OF THE LATE MIOCENE SUCCESSIONS OF AKTOPRAK BASIN (CENTRAL TURKEY): IMPLICATIONS FOR SEDIMENT SOURCE AND PALEOCLIMATES

ALI GÜREL

Department of Geology Engineering, Niğde University, 51200 Niğde, Turkey

Abstract—Late Miocene (Messinian) alluvial and lacustrine deposits characterize the so-called Kızılbayır Formation of the Aktoprak Basin (central Turkey) and consist of conglomerate, sandstone, mudstone, limestone, marl, and dolomite units. These sediments are composed mainly of feldspar, quartz, hornblende, diopside, olivine, serpentine, calcite, and dolomite with subordinate palygorskite, chlorite, smectite, and illite. Studies by scanning electron microscopy indicate that calcite and dolomite show both meniscus and micrite-sparite-type cements, characteristic of both vadose and phreatic zones. Chlorite, smectite, and illite are products of the alteration of the underlying Güney Formation with subsequent transportation by local streams into the Kızılbayır Formation, and therefore these are considered to be reworked materials. Authigenic palygorskite and dolomite formed as a result of the calcretion of mudstone-carbonate units under alkaline conditions, with high Si, Ca, and Mg activity, and low Al, originated from ophiolitic and carbonate units based on the increase in Ni and Co. The paragenesis and textural features of the minerals of the alluvial fan and lacustrine sediments determined in the study area indicate that precipitation probably occurred due to climate fluctuations ranging from arid and semi-arid to wet conditions.

Key Words—Alluvial Fan, Aktoprak Basin, Clay Minerals, Kızılbayır Formation, Lacustrine Sediments, Late Miocene, Palygorskite.

INTRODUCTION

Reconstructions of past climate changes have been based on information obtained from a variety of sources though lakes and lacustrine deposits have been particularly useful (Cock *et al.*, 1999). According to Torgersen *et al.* (1986), lakes frequently contain a variety of paleoenvironmental information that can reflect changes on local, regional, or global scales. Lakes are the product of physical interactions that operate over significant time scales and, as a result, may persist in the environment for substantial periods of time and produce fine-resolution records of change. Such changes can be better understood by employing data acquired from floral and faunal observations, and from sedimentological, mineralogical, and geochemical studies. Therefore clay mineralogy has become more significant in understanding the changes in paleoclimate conditions and sediment source.

In sediments, clay minerals may be originally detrital, diagenetic, or neoformed in non-marine successions (*e.g.* Singer, 1979). Numerous authors have studied historical clay mineral variations from different environments. In particular, non-marine, authigenic palygorskite and dolomite were studied by many researchers, *e.g.* Inglès and Anadón (1997) on the Eocene in the Pontils Group, SE Ebro Basin (Spain); Galán *et al.* (1994) on the Neogene–Quaternary sediments of the Carrion lacustrine basin (Ciudad Real, central Spain); Shadfan *et al*. (1985) on the Tertiary Formations of eastern Saudi Arabia; Khademi and Mermut (1998) on Oligo-Miocene palygorskite in gypsiferous Aridisols and associated sediments from central Iran; Karakaş and Kadir (1998) on the Neogene volcanoclastic sediments of Konya Basin (Turkey); and Enzel *et al.* (1999) on the Holocene environmental changes in the Thar Desert, northwestern India. In addition to those investigations, other authors have studied facies leading to the formation of clay minerals: *e.g.* Çağatay (1990) on clay mineral variation in paleomarine environments; Verrecchia and Le Coustumer (1996) on soil and paleosol environments; and Kaçmaz and Köktürk (2004) on hydrothermal solution environments.

The Aktoprak Basin covers 300 km^2 in the southern part of central Anatolia (Figure 1). Previous work on the study area and surrounding district was done by Oktay (1982), and by Nazik and Gökçen (1989) who investigated the stratigraphy, paleontology, and tectonics; Jaffey (2001), Clark and Robertson (2002, 2005), and Jaffey and Robertson (2005) worked on the sedimentology, geochemistry, petrography, and tectonic evolution of the area; Demirtaşlı *et al.* (1984) focused on the mining potential; and Gürel *et al.* (2007) concentrated on the sedimentological characteristics.

Each Anatolian lake basin has its own natural history, which evolved under the control of local, regional, and global factors (Erol, 1999). The diversity of these factors

* E-mail address of corresponding author:
agurel_1999@yahoo.com
DOI: 10.1346/CCMN.2008.0560607

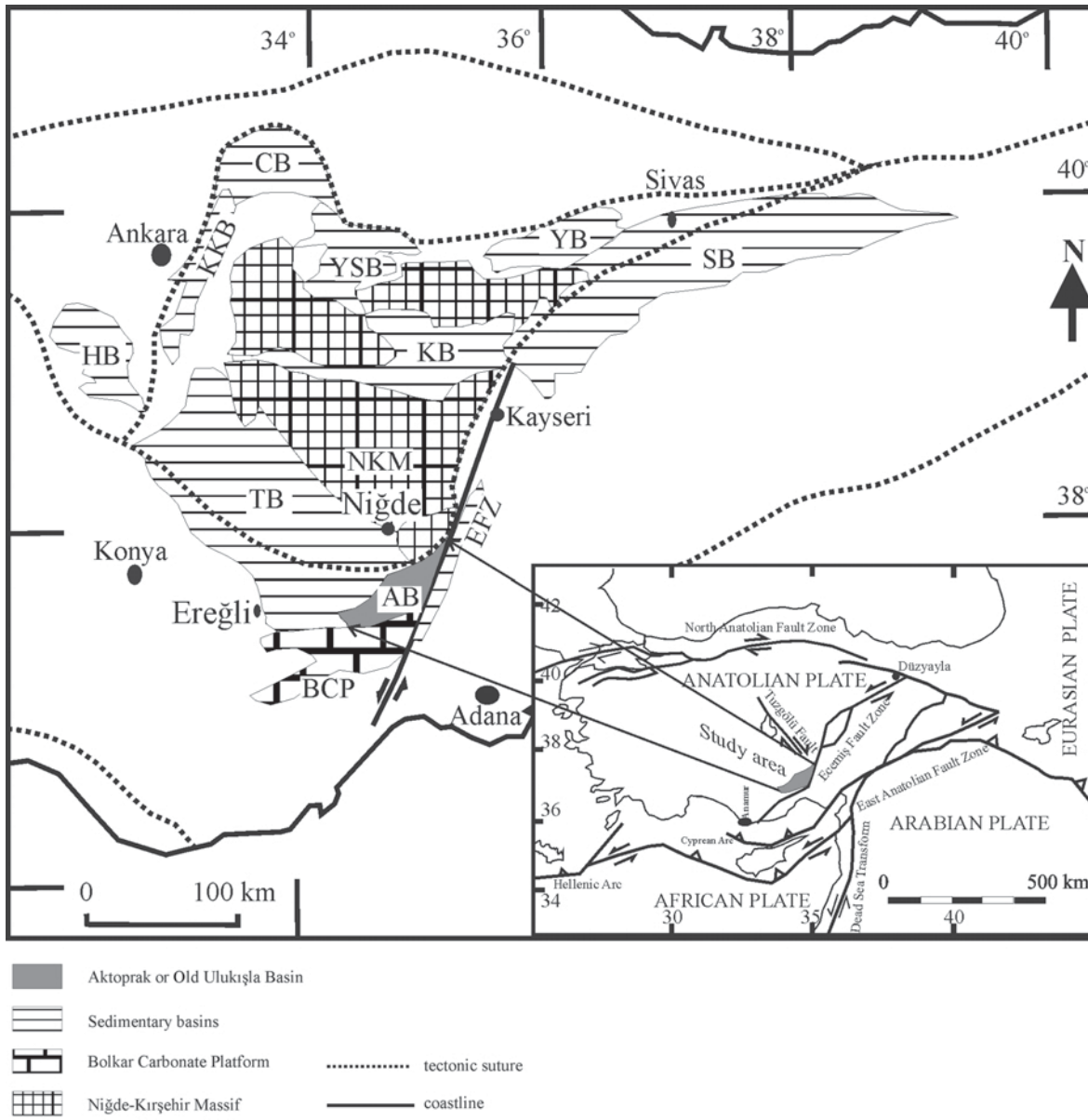

Figure 1. Major sedimentary basins and microcontinental units of Central Anatolia. The Bolkar Carbonate Platform (BCP) and the Niğde-Kırşehir Massif (NKM) are shown. (AB, Aktoprak Basin or old Ulukışla Basin; TB, Tuzgölü Basin; HB, Haymana Basin; KKB, Kırıkkale Basin; CB, Çankırı Basin; YSB, Yozgat-Sorgun Basin; KB, Kızılırmak Basin; YB; Yıldızeli Basin; SB, Sivas Basin; EFZ, Ecemiş Fault Zone) (redrawn and modified from Görür *et al.*, 1998; Clark and Robertson, 2005)

between the basin and mountains led to highly varied and contrasting conditions (Gürel and Yıldız, 2007). Some lakes show 'closed lake' and others 'open lake' character. The Aktoprak lake basin has features which are different from the central Anatolian basins and from other such basins on Earth. In addition, the Aktoprak Basin was fed by rivers from ophiolitic basement-rock areas, and sediment deposition took place in Messinian time under dry conditions in a very limited, closed basin.

No information is available on the vertical distribution of clay mineralogical properties in the fluvial-lacustrine sediments from Aktoprak Basin in relation to climatic changes during Late Miocene. The aims of this study were: (1) to investigate the mineralogical and geochemical properties of the calcareous fluvial-lacustrine sediments; (2) to determine the origin of various minerals and clay minerals in the sediments; and (3) to estimate climatic changes in the Aktoprak Basin on the basis of mineralogical and geochemical characteristics of the Aktoprak clayey and calcareous sediments. Furthermore, the sedimentology, mineralogy, and origin of paygorskite-dominated clay minerals and the formation of carbonate minerals such as calcite and dolomite in these sediments are discussed.

GEOLOGICAL SETTING

Central Turkey has undergone Neotectonic deformation since Oligo-Miocene times. Many faults and intracontinental basins in this region either formed or were reactivated during this period (Dirik and Göncüoğlu, 1996). The Ulukışla Basin consists of two entirely different basins, the older of Late Cretaceous to Lower Oligocene age, which contains ~5 km of sedimentary and volcanic rock (Figure 2, Jaffey and Robertson, 2005) and was deformed in the Late Eocene. This basin is unconformably overlain by the Oligo-Miocene basin. The younger Oligo-Miocene basin was distinguished (Jaffey and Robertson, 2005) as the Aktoprak Basin and it was separated from the older, well documented Ulukışla Basin.

The Ulukışla volcano-sedimentary units unconformably overlie the Late Cretaceous Alihoca ophiolite which was emplaced on the Bolkar Carbonate Platform (Figure 1). The volcano-sedimentary rocks in the Ulukışla Basin include: (1) the Sansartepe Formation which is composed of trachyandesitic pillow lavas and monzonitic shallow intrusives; (2) the Serenkaya Formation consisting of conglomerates overlain by cyclic graded and bedded gravel-sandstone-mudstone alternation; (3) the Başmakçı limestone consisting of pelagic limestone and reef limestone; (4) syenite and trachyte; (5) the Karatepe limestone consisting of reef limestone; (6) the Güney Formation that begins with gray mudstone-calciturbidite alternation at the base and continues toward the top with turbiditic sandstone; and finally (7) andesite and trachyte. According to Oktay (1982), the age of the Ulukışla units range from Late Cretaceous to Late Eocene (Figure 2).

The Aktoprak Basin in central Turkey is a >3000 m thick succession of Oligo-Miocene deposits, which includes the Zeyvegediği anhydrite and the Kurtulmuştepe-Kızılöz-Kızılbayır-Katrandedetepe Formations. During the Pliocene compressional events, the area corresponded to an elongate domain running parallel to the Niğde Fault Zone (NFZ; Figure 2) from the towns between Niğde and Ereğli (Figure 1). In the Aktoprak Basin, Paleogene-Neogene deposits exhibit a relatively smooth topography with respect to the older rocks. The sediment fill of the Aktoprak Basin overlies unconformably the Late Cretaceous-Late Eocene mixed siliciclastic, carbonate, and volcanogenic series of the Ulkışla Basin (Oktay, 1982; Clark, 2002; Figure 2).

The Paleogene-Neogene stratigraphy starts with the Zeyvegediği anhydrite and the Kurtulmuştepe Formation, both of Oligocene age. The Zeyvegediği anhydrite is ~800 m thick which consists of mud-supported anhydrite-selenite conglomerate interbedded with marls, thin bedded limestone and sandstone. The Kurtulmuştepe Formation, up to 900 m thick, consists mainly of marl-limestone intercalation. The Kızılöz Formation, up to 800 m thick and consisting of cross-bedded conglomerate, sandstone, and mudstone, formed mainly as braided river settings throughout the area. This formation is followed by local travertine indicating the presence of terrestrial conditions in the Middle Miocene, and marks a stratigraphic diastem or unconformity. The Late Miocene Kızılbayır Formation, which is the subject of this study, comprised ~130 m of sediments, consisting of alternating conglomerate, sandstone, and mudstone and intercalated with limestone, marl, lignite, and dolomite (Figure 2). The Katrandedetepe Formation, up to 100 m thick, consists of alternating marl and limestone. This formation underlies concordantly the Beştepeler Formation and the other Quaternary deposits. The Beştepeler Formation consists of fluvial sediments containing large-scale, cross-bedded and alternating, very loosely cemented gravel and sand.

MATERIALS AND METHODS

Field work was carried out using the existing geological maps of the Kolsuz, Kızılbayır, Katrandedetepe, and Gelinkayaları areas modified from the 1:100,000-scale map (Oktay, 1982). To identify the lateral and vertical distributions of clay minerals, four stratigraphic sections within the study area were examined (Figures 1–3).

Forty-five sediment samples, representative of the various facies of the Güney, Kızılbayır, Katrandedetepe, and Gelinkayaları sections, were analyzed with respect to their mineralogical characteristics by polarized-light microscopy (Olympus-BH-2 3M0548 Pol.), X-ray powder diffractometry (XRD) (Siemens D 5000, Diffrac. AT V. 3.1), and scanning electron microscopy equipped with energy dispersive X-ray microanalysis (SEM-EDX) (Noran, Cam scan, Pioneer TP 250). The XRD analyses were performed using CuKα radiation and a scanning speed of 1º2θ/min. Unoriented mounts of powdered whole-rock samples were scanned to determine the mineralogies of the bulk samples. Samples for clay analysis (<2 μm) were prepared by separation of the clay fraction by sedimentation, followed by centrifugation of the suspension after overnight dispersion in distilled water. The clay particles were dispersed by ultrasonic vibration for ~15 min. Four oriented specimens of the <2 μm fraction were prepared from each sample: air-dried; ethylene-glycol-solvated at 60ºC for 2 h; and thermally treated at 350ºC and 550ºC for 2 h. Semi-quantitative analyses of rock-forming minerals were obtained using the external standard method of Brindley (1980), whereas the relative abundance of clay mineral fractions was determined using their basal reflections and the mineral intensity factors of Moore and Reynolds (1989). Representative clay-dominated bulk samples were prepared for SEM-EDX analysis by adhering the fresh, broken surface of each rock sample onto an aluminum sample holder and coating with a thin film (350 Å) of gold using a Giko ion coater.

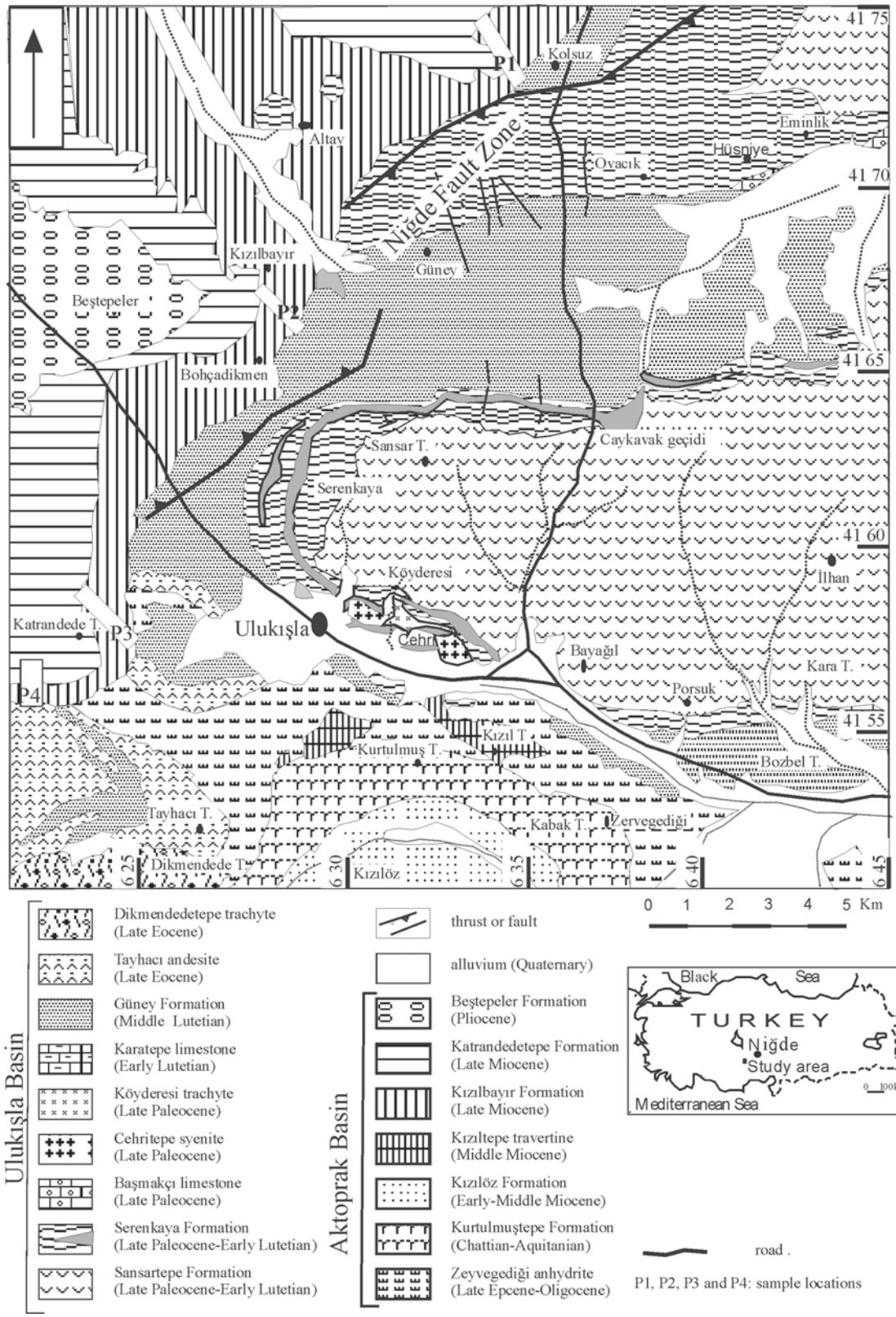

Figure 2. Simplified geological map of the Aktoprak Basin (redrawn and modified from: Oktay, 1982; Demirtaşlı *et al.*, 1984; Çevikbaş and Öztunalı, 1991).

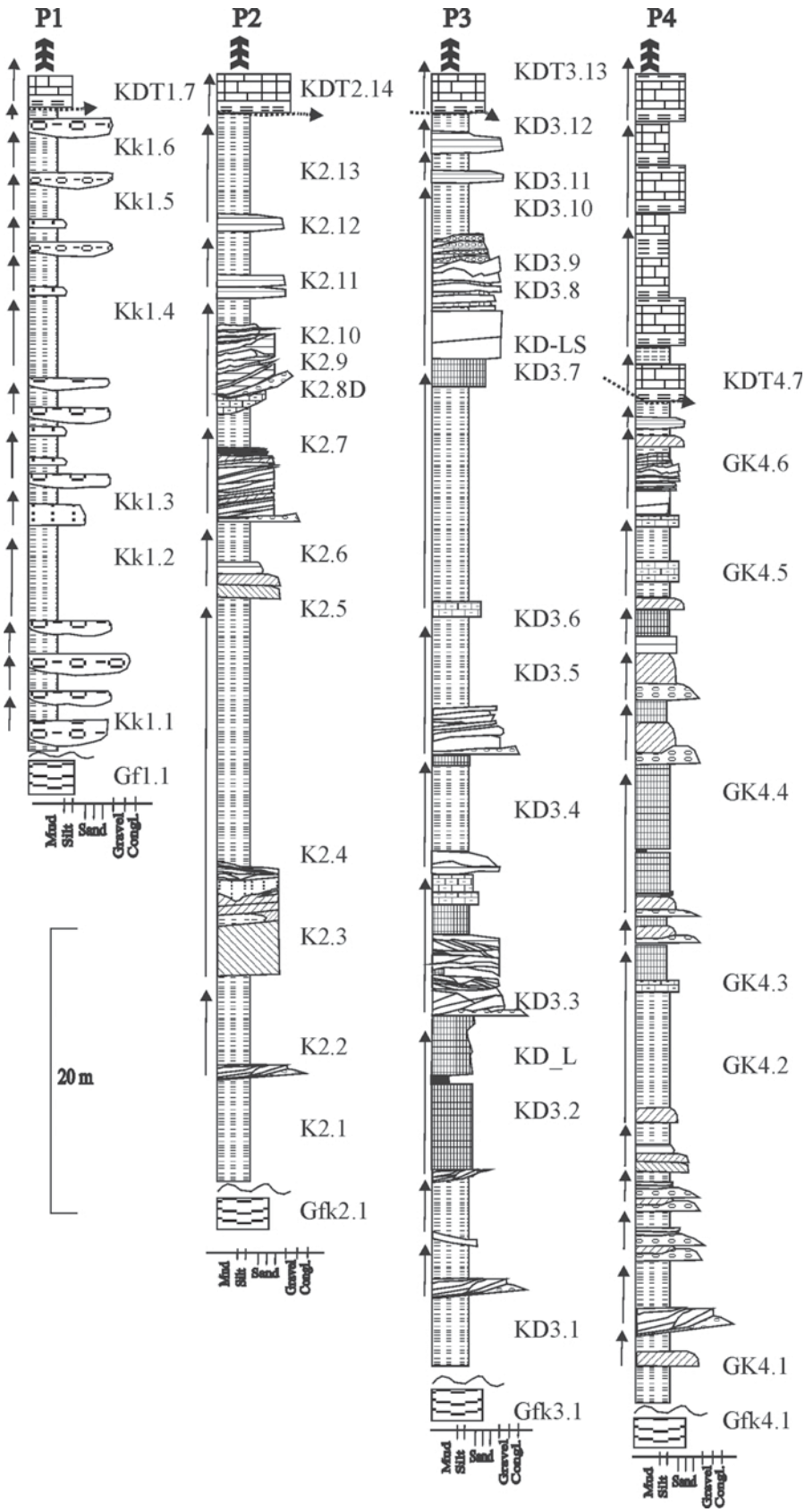
P1
P2
P3
P4
KDT1.7
Kk1.6
Kk1.5
Kk1.4
Kk1.3
Kk1.2
Kk1.1
Gf1.1
KDT2.14
K2.13
K2.12
K2.11
K2.10
K2.9
K2.8D
K2.7
K2.6
K2.5
K2.4
K2.3
K2.2
K2.1
Gfk2.1
KDT3.13
KD3.12
KD3.11
KD3.10
KD3.9
KD3.8
KD-LS
KD3.7
KD3.6
KD3.5
KD3.4
KD3.3
KD_L
KD3.2
KD3.1
Gfk3.1
KDT4.7
GK4.6
GK4.5
GK4.4
GK4.3
GK4.2
GK4.1
Gfk4.1
20 m
Mud
Silt
Sand
Gravel
Congl.

Chemical analysis of 25 representative samples (by inductively coupled plasma-atomic emission spectrometry) of clayey sediments, calcretes, and limestone-bearing samples, for major and trace elements, and using inductively coupled plasma-mass spectrometry for rare-earth elements (*REE*), were carried out at Acme Analytical Laboratories Ltd. (Canada). In these analyses, detection limits ranged from 0.01 to 0.1 wt.% for major elements, and 0.01−0.5 mg/kg for trace elements.

RESULTS

Petrography and diagenesis

Conglomerate source. The grain size of clasts in the area decreased to the northeast, around Kolsuz, Kızılbayır, Katrandedetepe, and Gelinkayaları (Figure 2). Therefore, most coarse-grained clasts were seen in the sections at Kolsuz and Kızılkbayır (Figure 3).

Clasts >1.6 cm in diameter were identified. Ophiolite-related clasts (gabbro, serpentine, radiolaria, and chert) are most abundant in the sections at Kolsuz and Kızılbayır, which were derived from Old-Ulukışla Basin, ophiolitic basement rocks, or from the Niğde Massif in the north and northwest. Limestone clasts are the second most abundant, and were transported from the Old-Ulukışla Basin. Greywacke, sandstone, and claystone clasts were also derived from the Old-Ulukışla Basin. Basalt, andesite, and diorite porphyry clasts were rare, and these were transported from Melendiz volcanic mountains (Aydin, 2008) or Old-Ulukışla Basin in the north and northwest.

The host clasts are well cemented, with primary pore space in the range 6−12%. The different sections of the Aktoprak Basin underwent different diagenetic processes. The Kolsuz and Kızılbayır sections show a simple diagenetic imprint and the clasts are coated by

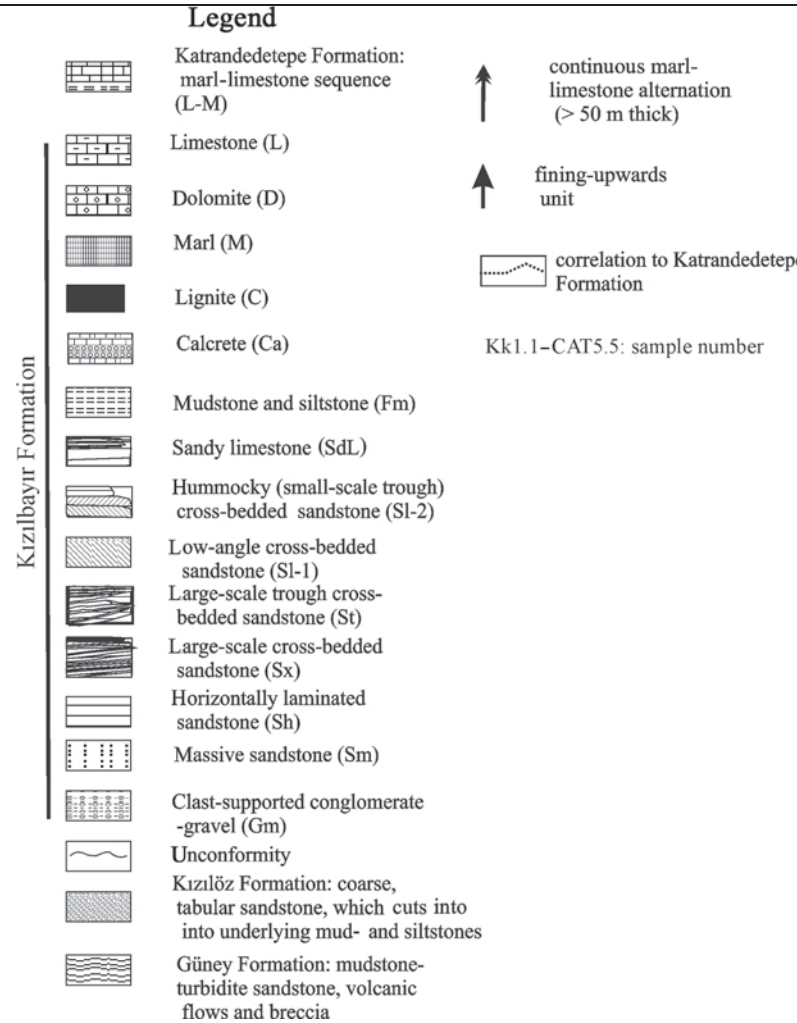

Figure 3 (*facing page and above*). Logged sections of the Kızılbayır and Katrandedetepe Formation, illustrating the principal lithofacies observed at: (P1) the Kolsuz, (P2) the Kızılbayır, (P3) the Katrandedetepe, and (P4) the Gelinkayaları localities (see Figure 2)

dark, film-like oxidation products such as Fe oxide and a late calcite spar, with detrital clay minerals filling the rest of the porosity.

Sandstone-siltstone unit. Detailed clast counting (based on 300 counts per thin section) was carried out in the Aktoprak Basin sediments. The sandstones in the sections of the area are comprised of quartz (microcrystalline), feldspars (K-feldspar and oligoclase), and lithic fragments (Figure 4C,D). For the lithic fragments, gabbro, serpentinite, quartzite, chert, limestone, mudstone, sandstone, greywacke, basalt, andesite, and diorite porphyry were determined (Figure 4C–E). A point count indicates that the quartz content of the sections decreases upward, whereas the feldspar and ophiolite-related lithic fragments contents increase. Other varieties of minerals include olivine, clinopyroxene (diopside), hornblende, serpentine, heavy minerals, and muscovite (Figure 4E,F).

Other varieties of clasts include clay lumps (glaebular structure). These are red in color and commonly rounded. Their size varies from 1 to 3 cm. Fragments of plant remains also occur in the sandstone. All the sandstones are red and some show characteristic white mottling, the size of which varies from 5 to 6 cm.

The host grains from the Late Miocene sandstone show a first coating of Fe oxide-micrite and acicular carbonate cement. Calcite cement in Fe oxide-micrite and acicular carbonate is a typical coating. The geometry indicates precipitation in the near-surface, phreatic-vadose environment. The remaining areas of sandstone-siltstone were precipitated later as a large, equant spar, drusy mosaic.

Finally, examination of thin sections of the conglomerate and sand-siltstone units showed that the host sediment in all samples consists of poorly sorted, subangular rock fragments, feldspars, quartz, hornblende, diopside, olivine, serpentine, heavy mineral grains, and various clay minerals, together with minor amounts of comminuted detrital carbonate allohems and gastropod remains in some levels.

Carbonate unit. The carbonate unit of Aktoprak Basin contains limestone, marl, sandy limestone, and calcrete. The limestone and marl shows a uniform micritic grain texture characteristic of calcic muds and sandflats currently formed subaqueously in shallow, fresh-water lakes. Uniform, micrite-dominated areas show local patches of spar with variably shaped open spaces in which calcite precipitated generally euhedral and subhedral mosaics. These show distinct phases of cementation, with micrite and acicular sparite occurring as an initial grain coating overlain by sparite towards the center of voids (Figure 4B). The host sediments in all samples consist of quartz and feldspar grains, together with small numbers of gastropods, bivalves, ostracods, and algae.

Sandy limestone contains quartz, ophiolite-related lithic fragments, and feldspar. These fragments are coated by micrite and acicular carbonate or a late calcite spar.

Many of the calcrete samples are brecciated, and in thin section, cavities and cracks are abundant. These are now filled by micrite-clay minerals, microsparite, or late calcite spars and display a variety of morphologies (Figure 3A, K fabric of Gile *et al.*, 1966).

BULK AND CLAY MINERALOGY

Context. Before concentrating our studies on the sedimentary Kızılbayır, Katrendedetepe Formation which spans the proposed Late Miocene sections in the Aktoprak Basin, preliminary investigations were carried out of 10 background analyses of clay-rich beds from the Kızılöz and Güney Formation below the study level (Figure 5, Table 1).

The Güney Formation, which is ~1000 m thick, consists of shale and greywacke. Shale sediments are composed of quartz, feldspar, calcite, and dolomite. Chlorite and illite are the predominant clay minerals, associated locally with accessory smectite. Greywacke sediments are composed of quartz, feldspar, calcite, and diopside. Chlorite is the predominant clay mineral, associated locally with accessory illite and smectite.

The Kızılöz Formation, which is ~800 m thick, is comprised of small- to large-scale cross-bedded conglomerates, sandstones, and mudstones. Mudstone sediments consist of quartz, feldspar, and diopside. Chlorite is the predominant clay mineral, locally associated with accessory illite and smectite.

The Kolsuz section (P1; Table 1)

Bulk mineralogy. The Kolsuz section is characterized by successions of red siliciclastic deposits >60 m thick and contains massive conglomerate, massive sandstone, and

Figure 4 (*facing page*). Photomicrographs of: (A) anastomosing fractures (light) in the calcrete body. The fragments appear to retain their shape, indicating that brecciation occurred *in situ* and that these lumps (a) have not been transported. The fractures are cemented by dolomite and palygorskite (a,b) (K3.9S, crossed polarized light), Scale bar = 0.5 mm. (B) Micritic limestone (algal mats, (a), showing distinct phases of cementation, with micrite and acicular sparite (b) occurring as an initial grain coating overlain by sparite towards the centers of the voids (c) (K3.9S, crossed-polarized light). (C) Ophiolite-related fragments such as serpentinite (s), quartzite (qu) and oligoclase (o) are healed by calcite cement (ca) (KG.3, crossed-polarized light). (D) Chert (ch), limestone (l), mudstone (m), and diorite porphyry (qd) cemented by alteration products and calcite (ca) (K3.12, crossed-polarized light). (E) Ophiolite-related minerals olivine (oli), diopside (d), and carbonate allocem, cemented by alteration products and calcite (KG.3, crossed-polarized light). (F) serpentinite (s), heavy minerals (hm), diorite porphyry, and chlorite (chl) cemented by alteration products and calcite (KG.3, crossed-polarized light).

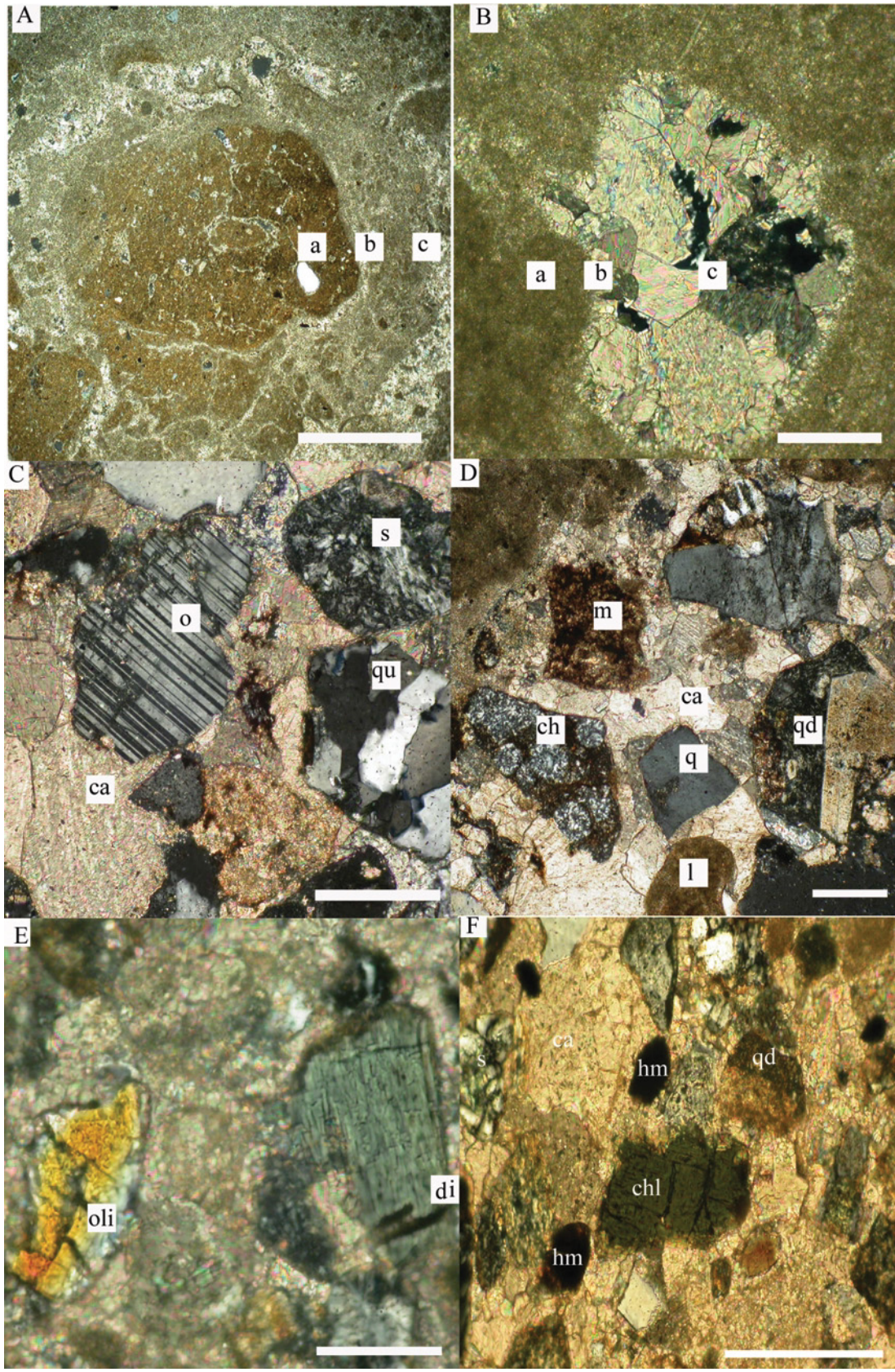
A
a
b
c
B
a
b
c
C
s
o
qu
ca
D
m
ca
ch
qd
q
l
E
oli
di
F
ca
s
hm
qd
chl
hm

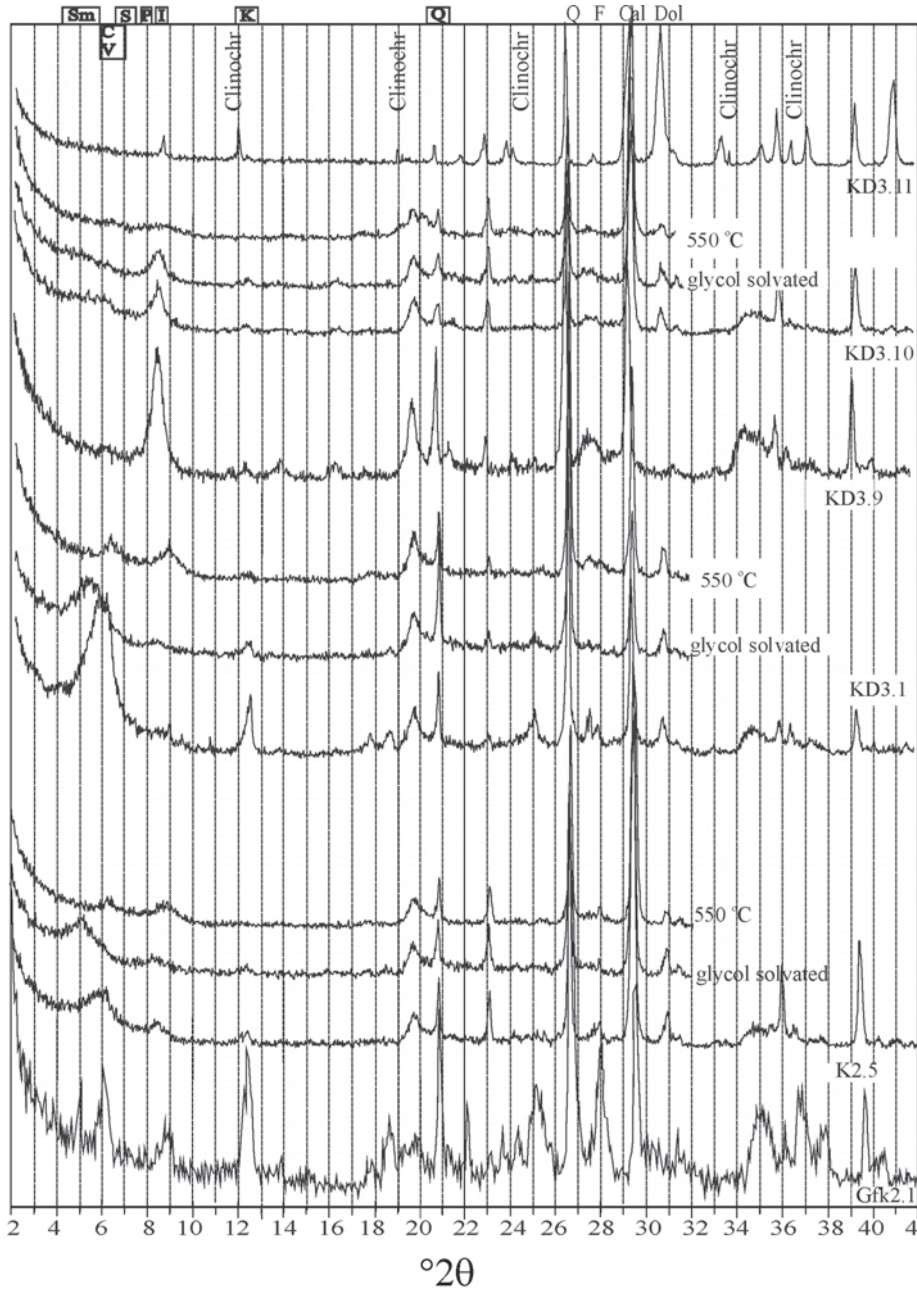

Figure 5. XRD patterns of the Aktoprak Basin clay-rich fractions. Sm: smectite; C: chlorite; V: vermiculite; S: sepiolite; P: palygoskite; I: illite; K: kaolinite; F: feldspar; Q: quartz; Cal: calcite; Dol: dolomite; clinochr: clinochrysotile (serpentine).

silt-mudstone. The mineralogy is characterized by small amounts and variable proportions of clay minerals, quartz, feldspar, and calcite. The proportion of carbonate is generally very large and these are more abundant in the upper part of the section independent of the lithology. This unit overlies a lacustrine limestone and a marl succession representing the transition from the Kızılbayır to the Katrandedetepe Formation. These sediments contain calcium carbonate minerals, mainly calcite, and locally associated with accessory clay minerals.

Clay mineralogy. Most clayey sediments are comprised of relatively homogeneous clay assemblages with dominant detrital chlorite, illite, and smectite.

The Kızılbayır section (P2; Table 1)

Bulk mineralogy. The Kızılbayır section is characterized by successions of red siliciclastic and limestone-dolomite deposits >80 m thick, and are composed of dominant reddish, massive to vaguely laminated silt-mudstone and subordinate carbonate beds, containing

Table 1. Mineralogical variation along stratigraphical sections of the Kızılbayır Formation, Aktoprak Basin.

	Rock type	smc	ill	chl	pal	ser	fds	px	cal	dol	an	qtz	op
P1													
Gf1.1	shale	acc	acc	++			++		+	acc		+++++	
Kk1.1*	mudstone	+	+	+			++		++			+++	
Kk1.2*	mudstone	+	+	+			++		++			+++	acc
Kk1.3*	mudstone	acc	+	+		acc	++		+++			+++	
Kk1.4	mudstone	+	acc	+		acc	+++		+++			++	
Kk1.5	mudstone	acc	+	+			++		+++	acc		+++	
Kk1.6	mudstone	+	+	+	acc	acc	++		+++			++	
Kdt1.7	limestone			acc	acc		acc		+++++			acc	
P2													
Gf2.1	shale	acc	+	++			+++	+	acc	acc		+++	
K2.1	mudstone	+	+	+			acc		++	+++	+	+	
K2.2	mudstone	+	acc	+			+		+++	acc		++++	
K2.3	mudstone	+	acc	+			+		+++	acc		++++	
K2.4	mudstone	++	acc	+			++		++	acc	acc	+++	acc
K2.5	mudstone	+	acc	+			+		+++	+		+++	
K2.6	mudstone	+	acc	+	+		+		+++	+		++	
K2.7	sandstone	+	+	acc	acc		+		+++	+		+++	
K2.8	dolomite	acc	acc	acc	+		acc		acc	+++++	+	acc	
K2.9	sandstone	acc	acc	acc	+	+	+	acc	++++	+	acc	++	
K2.10	sandstone	+	acc	acc	+		+	acc	+++++	+		++	
K2.11	mudstone	++	acc	acc	+		+	acc	+++++	acc		+	acc
K2.12	mudstone	++		acc	+		acc		+++	+		+++	
K2.13	mudstone	++		acc	+	acc	acc		+++	+		+++	
Kdt2.14	limestone			acc	acc				++++	+		acc	
P3													
Gfk3.1	greywacke	acc	acc	+		acc	+++	acc	+			+++++	
KD3.1	mudstone	++	acc	+	acc		++	acc	++	+		++	acc
KD3.2	marl	++	acc	+	+		acc	acc	+++	+		++	
KDD_L	lignite	acc					acc		+++++			acc	
KD3.3	marl	acc			acc		acc		+++++	acc		acc	
KD3.4	mudstone	+	acc		++		+		++	+++	+	+	
KD3.5	mudstone	+	acc	acc	++		+		++	+++	+	+	
KD36	limestone	acc			acc				+++++				
KD3.7	marl	+	acc	acc	+++		acc		+	++++	+	+	
KD-LS	sandstone	+		acc	acc	acc	acc		+++++	+	acc	+++	
KD3.8	limestone	acc			+				++++			acc	
KD3.9	Ca_red	acc		acc	+++				+++	++		++	
KD3.10	Ca_white	acc			+				++++			acc	
KD3.11	sandstone	acc	+	acc		+	+		++	+++		++	
KD3.12	mudstone	acc		acc	+++				+++++			++	
Kdt3.13	limestone	acc							+++++			acc	
P4													
GK 4.1	mudstone	+++	+++	+			+		+	acc		+	
GK 4.2	mudstone	++	+++	+	+		+		+	acc		+	
GK 4.4	marl	+	+	+	+		+		+	+		+	
GK 4.5	limestone	acc							+++++				
GK4.6	calcrete	acc			acc				+++++				
Kdt4.7	calcrete	acc			+++		+		++++	+		acc	

The locations of the samples are given in Figure 2: P1, P2, P3, and P4.
Symbols – smc: smectite, ill: illite, chl: chlorite, pal: palygorskite, ser: serpentine (clinochrysotile), fds: feldspar, px: pyroxene, cal: calcite, dol: dolomite, an: ankerite qtz: quartz, op: opal-CT
+: relative abundance of mineral phase, acc: accessory
*: Data sources: Kayalı *et al*. (unpublished)

massive conglomerates, cross-stratified sandstone, and mud-siltstone. The mudstone beds are dominated by quartz, calcite, and feldspar, with opal-CT occurring in small amounts on a few levels, especially the middle and upper parts of the section. The sandstones have a similar mineral content to the mudstone, but in addition, contain small amounts of diopside. The carbonate sediments of the section consist mainly of calcite or dolomite, and a small amount of the latter is ankerite.

Clay mineralogy. The silt-mudstone beds are dominated by smectite, followed by chlorite, palygorskite, and illite. The amounts of smectite and palygorskite increase in the upper part of the profile whereas the illite and chlorite contents decrease.

The Katrandedetepe and Gelinkayaları sections (P3 and P4; Table 1)

Bulk mineralogy. This lithofacies is characterized by successions of red siliciclastic and white carbonate deposits, which consist of massive conglomerate, horizontally stratified sandstone, large-scale cross-stratified sandstone, sandy limestone, mudstone, calcrete, lignite, marl, and limestone. In the Katrandedetepe and Gelinkayaları locations, the stratigraphic successions studied reach up to 80 m in thickness.

The mudstone and marl beds exhibit a mineralogy that is dominated by quartz, feldspar, calcite, and dolomite and a small proportion of the latter is ankerite. Limestone and white calcrete beds are dominated by calcite minerals associated locally with accessory quartz. The red calcrete beds consist of calcite, dolomite, and quartz. Sand beds exhibit a mineralogy that is dominated by quartz, feldspar, calcite, and dolomite, associated locally with accessory diopside.

Clay mineralogy. The mudstone-marl beds are dominated by palygorskite, followed by smectite, chlorite, and illite. Limestone and white calcrete samples yield the following clay minerals. Palygorskite is the most common clay mineral, whereas smectite is present in minor amounts. The red calcrete beds are dominated by palygorskite, followed by chlorite and smectite. The clay pockets in the sandstone beds are dominated by illite, with a subordinate amount of smectite, chlorite, and palygorskite.

Scanning electron microscopy (P1–P4)

Some samples contain localized evidence of pre-cementation alteration and post-cementation diagenetic alteration that can be investigated by SEM. Some of the fibrous clinochrysotile crystals are partially resorbed, resulting in oriented, irregular, bar-shaped remnants of clinochrysotile grains (Figure 6a). Relics of bar-shaped, irregular, and unaltered grains are coated by micrite, micro-sparite (isopachous rim of acicular phreatic cement), and late calcite spar cement fills the rest of the porosity (Figure 6a). Clinochrysotile was determined by optical microscopy and XRD methods.

On the other hand, feldspar crystals are highly resorbed in places (Figure 6b). Relict feldspar is cemented by carbonate and clay minerals such as detrital illite, chlorite, and platy smectite. These sediments also enclose coarse, rounded rock fragments related to the basement units (Figure 6b), and a thin section through the grain-coating cement in overlying rock fragments shows the relationship between the thin initial Fe oxide-micrite and acicular carbonate coating and later precipitated sparite cement (Figure 6c). Carbonate and detrital grains are partially dissolved, and intergranular grain dissolution porosity is created (Figure 6d). Micromorphological SEM images suggest that palygorskite fibers developed as irregular fibers in dissolution voids and between sediments (*e.g.* rhombohedral dolomite), as oriented fibers in anastomosing fractures in the calcrete body, and as palygorskite fibres up to ~1 μm in diameter (Figure 6f–k).

In the alluvial fan-lake margin sediments of the P1 and P2 sections in the Aktoprak Basin, the detrital material is cemented by carbonate and detrital clay minerals such as illite, chlorite, and smectite (Figure 6l).

Geochemistry

Representative chemical analyses of the samples Kk1.1–Kk1.3 of section P1, K2.2–K2.12 of section P2, and KD3.1–KD3.12 of section P3 are listed in Table 2 (mudstone as the basement rock of the Güney Formation: Gfk1.1, and limestone of Katrandedetepe Formation: KDT2.14).

These units are represented by values of SiO_2 (0.24–49.44%), Al_2O_3 (1.45–13.97%), Fe_2O_3 (0.07–8.10%), CaO (6.94–55.79%), MgO (0.90–10.13%), and LOI (12.30–43.10%). The loss on ignition (LOI) values are an important indicator of the clay and carbonate minerals content in the samples.

The mudstone samples in all profiles are characterized by small Al_2O_3 (1.45–13.97%), SiO_2 (0.24–49.44%), and K_2O (0.50–2.64) and large CaO (6.94–55.79%) and MgO (0.90–10.13%) values. Therefore, these values reflect a large calcite, dolomite, and ankerite content in the samples. The clay content decreases with increasing CaO (6.94–55.79%) and MgO (0.90–10.13%). Similar results were acquired when the mudstone samples were compared with the average global mudstone values (Wedepohl, 1984). The representative limestone and calcrete samples (KD3.4, KD3.8, and KD3.10) are enriched in CaO (42.02–55.79%) content and in terms of LOI value (36.40–43.10%), whereas the other oxides show depletion. The clay-rich sediments were depleted, with Na_2O (0.03–1.72), K_2O (0.50–2.64), and P_2O_5 (0.05–0.17).

The clay-rich sediments of the Kızılbayır Formation are enriched with trace elements such as Sr (270–749 ppm) and Cu (19–177 ppm), in comparison to the average global mudstone values (Table 2). The

Table 2. Chemical result of the different lithologies in the study area.

	P1					P2							
Element (%)	Gfk1.1* shale	Kk1.1* mudst.	Kk1.2* mudst.	Kk1.3* mudst.	KDT limest.	K2.2 mudst.	K2.3 mudst.	K2.4 mudst.	K2.6 mudst.	K2.10 sandst.	K2.11 mudst.	K2.12 mudst.	KDT2.14 limest.
SiO_2	60.50	46.50	48.57	49.12	9.90	46.58	49.44	48.40	45.58	32.33	33.89	33.82	5.64
TiO_2	0.80	0.66	0.76	0.47	0.11	0.66	0.20	0.20	0.66	0.34	0.39	0.30	0.06
Al_2O_3	17.10	12.74	13.97	9.46	2.35	11.81	5.80	5.60	12.81	4.86	8.16	5.94	1.45
ΣFe_2O_3	6.50	7.28	8.10	4.24	0.94	5.99	3.47	4.47	6.30	4.44	5.38	5.34	0.69
MnO	0.2	0.14	0.14	0.15	0.14	0.14	0.14	0.18	0.15	0.07	0.08	0.06	0.16
MgO	2.5	4.68	5.09	2.90	1.85	5.28	2.38	2.56	5.58	5.62	4.36	7.36	4.86
CaO	1.7	9.37	6.94	15.04	45.04	11.30	18.45	18.00	11.39	25.19	21.00	20.97	45.61
Na_2O	1.4	0.96	1.10	1.72	<0.01	1.46	1.10	1.10	1.46	0.30	0.18	0.38	0.03
K_2O	3.1	2.31	2.64	1.65	0.33	1.96	0.87	0.87	1.96	0.53	0.97	0.50	0.15
P_2O_5	0.1	0.06	0.15	0.10	0.03	0.16	0.05	0.05	0.17	0.34	0.05	0.06	0.05
Cr_2O_3	0.072	0.028	0.028	0.029	0.024	0.025	0.053	0.041	0.043	0.174	0.044	0.088	0.010
LOI	5.9	15.10	12.30	15.00	39.3	14.40	17.90	18.30	14.31	25.9	25.40	24.90	41.2
Total	99.80	99.97	99.95	100.02	99.99	99.93	99.97	99.95	99.94	99.92	100.04	99.89	100.00
TOT/C	n.a.	2.07	1.54	3.31	10.39	2.60	4.13	3.93	9.80	5.52	4.74	4.99	11.11
TOT/S	n.a.	0.03	0.03	0.01	0.03	0.03	0.13	0.18	0.15	0.01	0.02	0.02	0.04
ppm													
Ba	409	153	340	374	129	288	176	151	290	75	110	77	37
Cu	55	177	54	44	<20	59	<20	<20	65	40	<20	43	<20
Zn	103	95	121	55	<20	84	30	39	86	51	100	48	<20
Ni	52	196	224	109	66	162	273	271	167	413	296	522	70
Co	27	<20	25	<20	<20	21	<20	<20	28	21	<20	27	<20
Sr	18	270	252	372	336	437	378	391	443	350	412	591	550
Zr	152	111	161	133	29	125	20	22	128	84	65	36	<10
Ce	n.a.	52	76	46	<20	93	<20	<20	98	24	35	39	<20
Y	119	20	27	21	12	24	14	13	27	16	14	12	<10
Nb	13	<10	18	<10	<10	21	<10	<10	19	<10	<10	<10	<10
Sc	18	19	20	12	2	16	7	10	17	11	12	15	2
Ta	n.a.	<20	<20	<20	<20	<20	<20	<20	<20	<20	<20	<20	<20

	P3												
Element (%)	KD3.1 greyw.	KD3.2 marl	KD_L lignite	KD3.3 mudst.	KD3.4 limest.	KD3.5 mudst.	KD3.6 Marn	KD3.8 limest	KD3.9 Ca_red	KD3.10 Ca_white	KD3.10 Ca-lamina	KD3.12 mudst.	T-S**	S***
SiO_2	46.36	37.18	33.18	44.25	0.24	30.72	32.18	1.48	14.38	10.66	9.90	34.38	58.90	33.68
TiO_2	0.63	0.56	0.59	0.58	<0.1	0.35	0.40	0.01	0.17	0.11	0.11	0.40	0.75	0.00
Al_2O_3	11.07	10.33	12.33	11.14	0.10	7.51	7.10	0.30	3.00	2.01	2.53	8.81	16.70	1.19
ΣFe_2O_3	8.59	6.54	6.53	8.65	0.07	5.69	4.72	0.21	1.39	1.43	0.94	5.51	6.65	10.08
MnO	0.07	0.08	0.20	0.09	0.05	0.08	0.07	0.07	0.06	0.01	0.04	0.07	0.09	0.13
MgO	5.89	5.75	5.73	5.93	0.45	7.90	10.13	0.90	1.75	1.87	1.85	4.82	2.60	40.77
CaO	7.57	15.17	13.15	8.47	55.79	18.34	16.58	53.74	42.02	45.00	45.04	19.46	2.20	0.45
Na_2O	0.19	0.07	0.02	0.14	0.01	0.06	0.01	<0.1	<0.01	<0.01	<0.10	0.03	1.60	0.00
K_2O	1.24	1.20	1.28	1.35	<0.02	0.83	0.86	0.03	0.52	0.25	0.33	1.12	3.60	0.00
P_2O_5	0.07	0.13	0.10	0.07	0.03	0.07	0.06	0.02	0.04	0.07	0.03	0.08	0.16	0.02
Cr_2O_3	0.061	0.043	0.120	0.075	0.03	0.061	0.046	0.008	0.056	0.038	0.024	0.050		0.23
LOI	18.00	22.70	26.70	19.15	43.10	28.1	27.6	43.10	36.40	38.20	39.30	25.10	6.3	13.09
Total	99.89	99.93	99.81	99.82	99.89	99.85	99.94	99.93	99.86	99.74	99.99	99.93	99.43	100.3
TOT/C	1.93	3.43	19.45	2.38	12.43	5.18	5.42	12.03	9.36	10.00	10.39	4.31	n.a.	n.a.
TOT/S	0.002	0.03	0.18	0.003	0.01	0.03	0.04	0.02	0.04	0.02	0.03	0.01	n.a.	n.a.
(ppm)														
Ba	173	144	152	156	24	98	160	25	79	54	129	106	460	4
Cu	46	65	72	47	<20	51	33	20	<20	32	<20	<20	45	5
Zn	87	97	86	81	<20	73	38	<20	<20	<20	<20	68	95	71
Ni	502	583	587	512	<20	530	339	<20	93	106	66	313	68	4998
Co	39	49	55	42	<20	43	29	<20	<20	<20	<20	24	19	35
Sr	195	408	390	205	275	248	749	343	397	504	336	243	n.a.	9
Zr	81	63	60	89	<10	44	50	<10	37	38	29	58	160	5
Ce	<20	23	28	<20	<20	34	<20	58	<20	30	<20	<20	n.a.	n.a.
Y	18	20	26	21	<10	18	16	<10	13	11	12	16	n.a.	<1
Nb	<10	12	10	<10	<10	<10	<10	<10	<10	14	<10	<10	n.a.	2
Sc	19	18	15	17	<1	14	12	<1	4	3	2	14	n.a.	n.a.
Ta	<20	<20	<20	<20	<20	<20	<20	<20	<20	<20	<20	<20	n.a.	n.a.

Data sources: * Kayalı *et al*. (unpublished); ** Wedepohl (1984); *** Yalçın and Bozkaya (2004); n.a. = data not available; mudst: mudstone, sandst: sandstone; limest: limestone; greyw: greywacke; T-S: terrigenous shale; S: serpenitinite from central Anatolia.

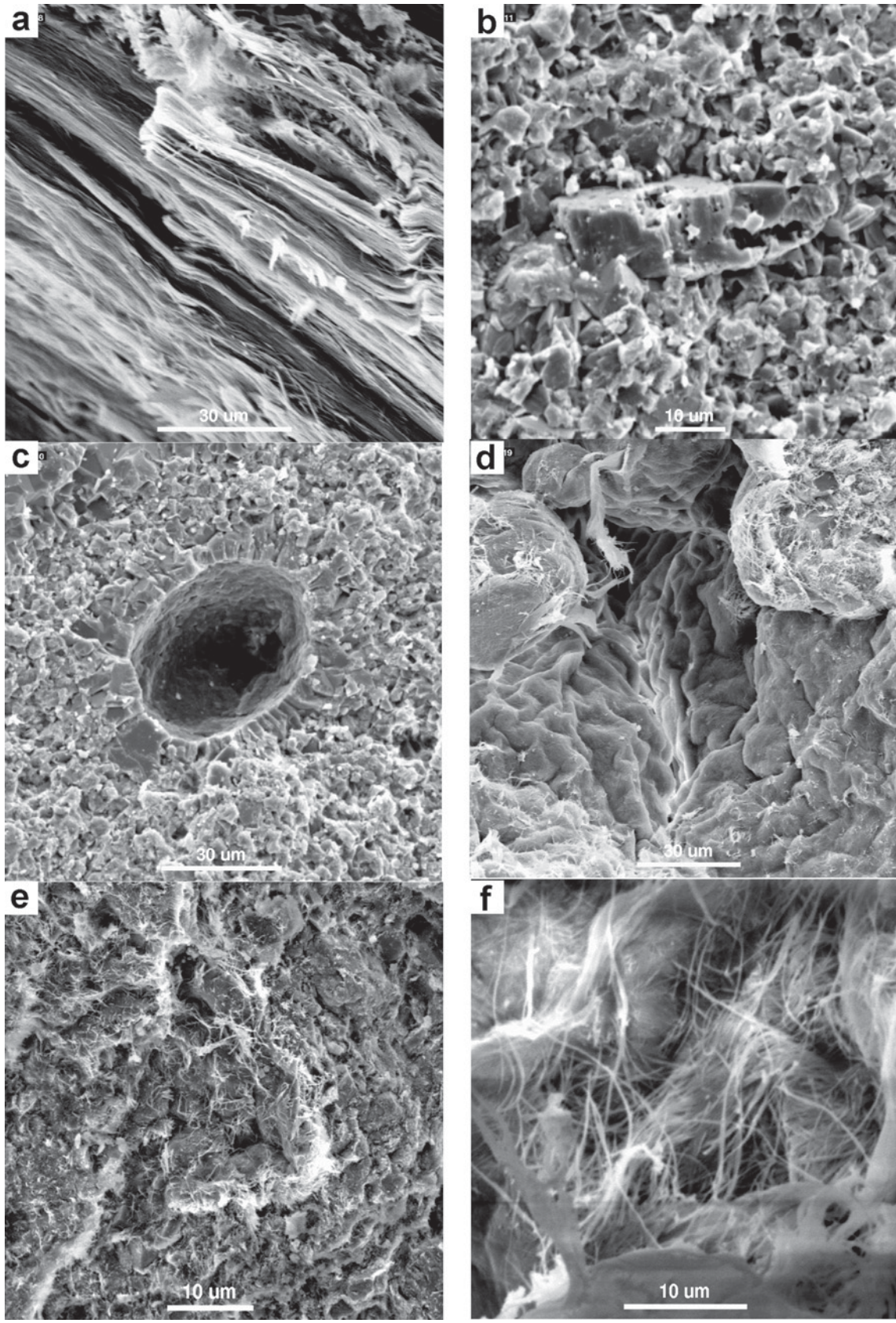
a
30 um
b
10 um
c
30 um
d
30 um
e
10 um
f
10 um

amount of Ni (109−587) and Co (19−55) present is greater than that of average global mudstone values (Wedepohl, 1984). The Ba and Zn values increase in the P1 section relative to the P2 and P3 sections. Ophiolitic units of central Anatolia are rich in MgO, Fe_2O_3, and Ni (Table 2, Yalçın and Bozkaya, 2004).

DISCUSSION

Source of sediments

The source areas of gravels consist of ophiolite-related rocks, accessory basalt, andesite, quartzite, diorite porphyritic rocks, and sedimentary rocks such

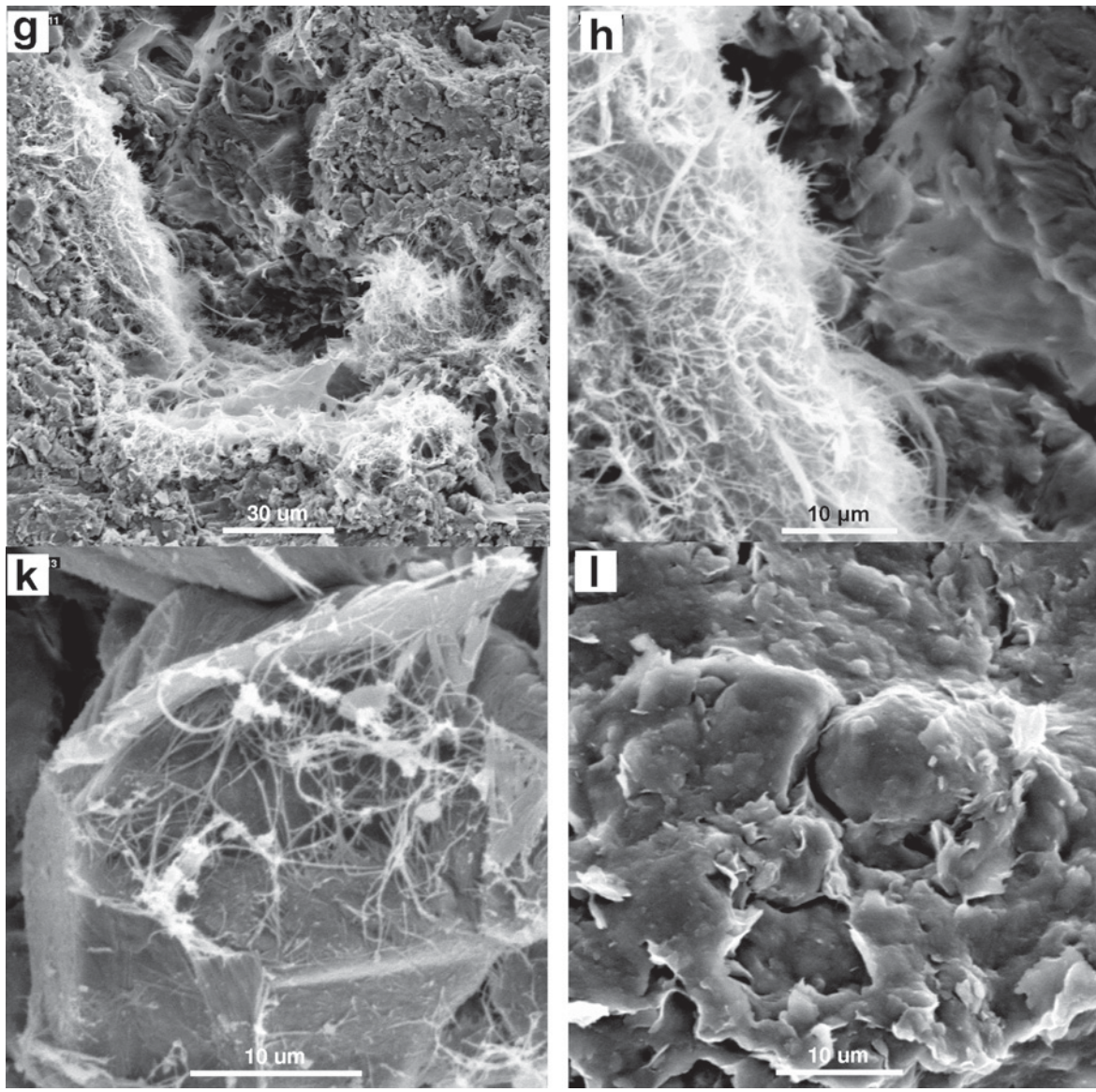

Figure 6 (*facing page and above*). SEM images showing the Aktoprak Basin sediment characteristics: (a) resorbed clinochrysotile (serpentine) crystals covered or cemented by clay and carbonate minerals (sample K3.9S); (b) dissolution features on feldspar grain-coating sparite cement and clay minerals; image of detrital illite, chlorite, and smectite plate (sample K3.7); (c) section through grain-coating cement overlying rock fragments showing the relationship between the thin, initial Fe oxide-micrite and acicular carbonate coating and later precipitated sparite cement (sample K3.9S); (d) partially dissolved calcite and detrital grains, such that intergranular grain dissolution porosity is created, together with calcified root hairs (up to 2 µm in diameter and 20 µm long, sample K3.9S); (e) anastomosing fractures (light) in the calcrete body filled by authigenic fibrous palygorskite networks (sample K3.9S); (f) close-up view of authigenic fibrous palygorskite; (g) authigenic fibrous palygorskites are partially filling secondary porosity and fractures (sample K3.9S); (h) close-up view of palygorskite mats; (k) close-up view of authigenic fibrous palygorskite networks and rhombohedral dolomite in dissolution voids; (l) image of detrital illite, chlorite, and smectite plate (sample K3.7).

as greywacke, sandstone, mudstone, and limestone, derived from the Niğde metamorphic area, the Alihoca ophiolitic zone, and the Güney Formation with Karatepe limestone of the Ulukışla Basin to the west. Quartz, feldspars, hornblende, olivine, diopside, serpentine (clinochrysotile), heavy minerals, and opal-CT type detrital materials also originated from the same source area.

Detrital clay assemblages of the Kızılbayır Formation mainly contain chlorite, smectite, and illite. These three minerals are detrital and they reflect the erosion of chlorite-, smectite-, and illite-rich sedimentary rocks cropping out close to the sedimentary basin. Those clay minerals have a common occurrence in the Güney Formation consisting of the basement of the Aktoprak Basin, a successor basin of the Ulukışla Basin (Table 1, Gf1.1–Gf3.1). These basement rocks were weathered extensively during the Late Miocene and transported to the Aktoprak Basin where they were redeposited. Therefore, the detrital clay minerals were derived from the reworked Güney Formation in the area (Gürel and Kerey, 2007).

All of the Kızılbayır Formation is enriched in calcite, with subordinate amounts of dolomite and ankerite. Lateral textural variation in the carbonate-rich units suggests that carbonate accumulation was controlled by local drainage conditions. The carbonate-rich units are developed in two ways. (1) The first is as a result of carbonate-rich subsurface waters flowing laterally through alluvial deposition. Observations from the study area show that the lacustrine basin is closely controlled hydrologically by the movement of $CaCO_3$-charged subsurface water, through weathered Ulukışla Basin sediments. The Alihoca ophiolitic zone and Niğde metamorphic rocks serve as a key carbonate source. (2) In the second, the carbonate host rock and detrital grains of limestone or carbonate allochems may have resulted from alteration of other carbonate sources within the evaporitic environment.

Intergranular spaces are filled as a result of carbonate precipitation in two stages: (1) the initial micrite and micro-sparite (isopachous rim of acicular phreatic cement) grain coating was subsequently overlain by sparite, which is the dominant cement throughout the profile; (2) longer periods of crystal growth took place under moist conditions at the bottom of the profiles allowing the development of bigger sparite. In contrast, in the upper part of the same section, micrite and micro-sparite dominated due to wetting and drying as the water table fluctuated. This fluctuation resulted subsequently in the formation of authigenic palygorskite in pore spaces during dolomitization (Karakaş and Kadir, 1998). Sand, clay, and carbonate-rich units accompany palygorskite in this basin and these altogether represent a more stable, low-energy environment. Dolomite and palygorskite precipitation is probably an important diagenetic process in the clay-rich units. The clusters of dolomite and palygorskite crystals are primarily euhedral aggregates, some of which show apparent multiple stages of crystallization. Single crystals of dolomite also occur dispersed among palygorskite fibers. Compilation of the entire set of data from the Kızılbayır Formation shows a regular increase in palygorskite at the top of each profile, which indicates that the increase in aridity probably continued to the end of Messinian time.

In summary, the occurrence of palygorskite in sections of the Aktoprak Basin, controlled by physico-chemical-environmental conditions, has been recognized in the present study. The large Ni, Co, Fe_2O_3, MgO, and CaO values suggest that the lake area was fed by rivers and ground water rich in alkaline ions under drought conditions (Singer, 1984), which originated from extensive weathering of ultramafic rocks and limestone (Table 2). An environment rich in Si and Mg with high pH, however impoverished in Al and Fe, helps the formation of palygoskite and dolomite (Singer, 1984). Those minerals precipitated due to changes in the chemical condition of the water that circulated within the anastomosing fractures (calcretion of mudstone-carbonate units; Lang *et al*., 1990). Therefore, mudstone, sandstone, limestone, and calcrete-dominated sediments throughout all levels of the profiles are palygorskite-bearing, associated with abundant dolomite that could be formed either during dolomitization or by direct precipitation. The occurrence of palygorskite associated with dolomite in Neogene volcaniclastic sediments of the Konya Basin was also reported by Karakaş and Kadir (1998). The formation of palygorskite in the Eocene–Miocene basin was widely reported (Weaver and Beck, 1977; Rodas *et al.*, 1994; Inglès and Anadón, 1997).

Paleoclimatic conditions and implications

Observations of the clay minerals from four vertical profiles of Late Miocene age have provided information about the environment of sedimentation and climatic conditions that prevailed across the Late Miocene in the Aktoprak Basin. Clay minerals, feldspars, and ophiolite-related minerals derived from the basement rock are subordinate, indicating the predominance of chemical weathering over physical weathering. The presence of palygoskite and dolomite in very shallow-lake environments may represent arid and semi-arid conditions at or near the Late Miocene sedimentation environment (Weaver, 1989; Chamley, 1989; Gürel and Kerey, 2007).

A global warming trend in the Late Miocene has been documented in the literature, including the time interval of the Messinian crises that led to the evaporation of the Mediterranean Sea (Rouchy and Caruso, 2006; Hardie and Lowenstein, 2004). In central Anatolia, the Late Miocene paleoclimate is interpreted as having been dry and wet-warm in temperature, based on the floral diversity of various pollen data of the central Anatolian sedimentary successions (Görür *et al.*, 1995;

Akgün *et al.*, 1995). These observations of the Aktoprak Basin are also supported by the chemical and mineralogical data of the clay minerals acquired throughout this investigation.

CONCLUSIONS

(1) In the non-marine conglomerate-sandstone-mudstones and carbonate units from the Late Miocene alluvial and lacustrine deposits of the Aktoprak Basin (central Anatolia), the minerals recognized are: (a) detrital clay minerals – illite, chlorite, smectite; (b) authigenic clay minerals – palygorskite; (c) authigenic carbonates – dolomite and ankerite; (d) diagenetic carbonates – calcite and dolomite; (e) carbonate rock fragments – limestone, carbonate allochem; (f) other rock fragments – gabbro, serpentinite, quartzite, chert, mudstone, sandstone, greywacke, basalt, andesite, and diorite porphyry, and (g) other silicates – quartz, feldspars, clinochrysotile, diopside, and opal-CT.

(2) The distribution of detrital minerals and the other rock fragments indicates the composition of the source area and their occurrence in the Aktoprak Basin during the Late Miocene. These minerals and lithic fragments have been found widely in the Güney Formation in the basement of the Aktoprak Basin, a successor basin of the Ulukışla Basin. Materials transported to the basin during the Late Miocene were subjected to various weathering processes, but partial weathering appears to have been prevalent, resulting in the common presence of detrital clays minerals within the Kızılbayır Formation.

(3) Sedimentary materials are cemented as a result of step-wise diagenetic processes within a lacustrine sedimentary basin. The calcrete and mudstone units show anastomosing fractures. The mud-rich lump fragments are largely maintained in shape, indicating that the brecciation occurred *in situ*, and not as a result of transportation. The fractures are cemented by dolomite and palygorskite. Authigenic dolomite and palygorskite form only in shallow-lake environments while detrital clay and carbonate minerals are found in the alluvial fan environment.

(4) The ophiolitic basement rocks and limestone crop out widely in the area and are the main source of Fe, Mg, and Ca, which were supplied to the lake environment leading to the formation of authigenic palygorskite and dolomite.

(5) The Aktoprak Basin can be represented as a hydrologically closed-lake system during the Late Miocene because of the presence of the carbonate and evaporate minerals in this area.

ACKNOWLEDGMENTS

The author is indebted to two reviewers for their comments and suggestions and to Associate Editor, Professor W. Huff (University of Cincinnati), all of whom helped to improve the quality of the manuscript. The author is also grateful for reviews of an early draft of the manuscript by Professor Rudolf Almann, Dr Andreas Schaper, Heinz Jepsen, Michal Helwig (Marburg University, Germany), Professor Selahattin Kadir (Eskişehir, Osmangazi University, Turkey), and Dr Emin Çiftçi (Niğde University, Turkey).

REFERENCES

Akgün, F., Olgun, E., Kuşcu, I., Toprak, V., and Göncüoğlu, M.C. (1995) New data on the stratigraphy, depositional environment, and real age of the Oligo-Miocene cover of the central Anatolian crystalline complex. *Bulletin of Turkish Association of Petroleum Geology*, **6**, 51–68 (in Turkish with English abstract).

Aydin, F. (2008) Contrasting complexities in the evolution of calc-alkaline and alkaline melts of the Nigde volcanic rocks, Turkey: textural, mineral chemical and geochemical evidence. *European Journal of Mineralogy*, **20**, 101–118.

Brindley, G.W. (1980) Quantitative X-ray mineral analysis of clays. Pp. 411–438 in: *Crystal Structures of Clay Minerals and their X-ray Identification* (G.W. Brindley and G. Brown, editors). Monograph **5**, Mineralogical Society, London.

Chamley, H. (1989) *Clay Sedimentology.* Springer Verlag, New York, 623 pp.

Clark, M. (2002) The latest Cretaceous–Early Tertiary Ulukişla Basin, S. Turkey: Sedimentation and tectonics of an evolving Tethyan suture zone. PhD thesis, University of Edinburgh, UK, 375 pp.

Clark, M. and Robertson, A.H.F. (2002) The role of the Early Tertiary Ulukışla Basin, southern Turkey, in suturing of the Mesozoic Tethys Ocean. *Journal of Geological Society*, **159**, 673–690.

Clark, M. and Robertson, A.H.F. (2005) Uppermost Cretaceous–Lower Tertiary Ulukişla Basin, south-central Turkey: sedimentary evolution of part of a unified basin complex within an evolving Neotethyan suture zone. *Sedimentary Geology*, **173**, 15–51.

Cock, B.J., Williams, M.A.J., and Adamson, D.A. (1999) Pleistocene Lake Brachina: a preliminary stratigraphy and chronology of lacustrine sediments from the central Flinders Ranges, South Australia. *Australian Journal of Earth Sciences*, **46**, 61–69.

Çağatay, M.N. (1990) Palygorskite in the Eocene rocks of the dammam dome, Saudi Arabia. *Clays and Clay Minerals*, **38**, 299–307.

Çevikbaş, A. and Öztunalı, Ö. (1991) Ore deposits in the Ulukışla-Çamardı (Niğde) Basin, *Jeoloji Mühendisliği Dergisi*, **39**, 22–40 (in Turkish with English abstract).

Demirtaşlı, E., Turhan, N., Bilgin, A.Z., and Selim, M. (1984) Geology of the Bolkar Mountains. Pp. 125–141 in: *Geology of the Taurus Belt* (O. Tekeli and M.C. Göncüoğlu, editors). Proceedings of the International Symposium. *Maden Tetkik ve Arama Dergisi*.

Dirik, K. and Göncüoğlu, M.C. (1996) Neotectonic characteristics of central Anatolia. *International Geology Review*, **38**, 807–817.

Enzel, Y., Ely, L.L., Mishra, S., Ramesh, R., Amit, R., Lazar, B., Rajaguru, S.N., Baker, V. R., and Sandler, A. (1999) High-Resolution Holocene environmental changes in the Thar Desert, northwestern India. *Science*, **284**, 125–128.

Erol, O. (1999) A geomorphological study of the Sultansazlığı lake, central Anatolia. *Quaternary Science Reviews*, **18,** 647–657.

Galán, E., Mesa, J.M., and Sanchez, C. (1994) Properties and applications of palygorskite clays from Ciudad Real, Central Spain. *Applied Clay Science*, **9**, 293–302.

Gile, L.H., Peterson, F.F., and Grossman, R.B. (1966)

Morphological and genetic sequences of carbonate accumulation in desert soils. *Soil Science*, **101**, 347–360.

Görür, N., Sakınç, M., Barka, A., Akkök, R., and Ersoy, S. (1995) Miocene to Pliocene palaeogeographic evolution of Turkey and its surroundings. *Journal of Human Evolution*, **28**, 309–324.

Görür, N., Tüysüz, O., and Şengör, A.M.C. (1998) Tectonic evolution of the central Anatolian basins. *International Geology Review*, **40**, 831–850.

Gürel, A. and Yıldız, A. (2007) Diatom communities, lithofacies characteristics and palaeoenvironmental interpretation of Pliocene diatomite deposits in the Ihlara-Selime plain (Aksaray, Central Anatolia, Turkey). *Journal of Asian Earth Sciences*, **30**, 170–180.

Gürel, A. and Kerey, E.I. (2007) Palaeoenvironmental reconstruction of Upper Miocene alluvial fan to cyclic shallow lacustrine depositional system in the Aktoprak Basin (central Anatolia, Turkey). *The 4th International Association of Limnogeology (IAL) Conference, Barcelona*, Volume **1**, p. 62.

Gürel, A., Çiftçi, E., and Kerey, I.E. (2007) Sedimentological characteristics of the Çukurbağ Formation deposited along the Ecemiş Fault Zone (Central Anatolia, Turkey). *Geological Society of India*, **70**, 59–72.

Hardie, L.H. and Lowenstein, T.K. (2004) Did the Mediterranean Sea dry out during the Miocene? A reassessment of the evaporite evidence from DSDP Legs 13 and 42A Cores. *Journal of Sedimentary Research*, **74**, 453–461.

Inglès, M. and Anadón, P. (1997) Relationship of clay minerals to depositional environment in the non-marine Eocene Pontils Group, SE Ebro Basin (Spain). *Journal of Sedimentary Petrology*, **61**, 926–939.

Jaffey, N. (2001) The Cenozoic evolution of the strike-slip Ecemis Fault Zone and its implications for the mechanism of tectonic escape in Anatolia. PhD thesis, University of Edinburgh, UK, 393 pp.

Jaffey, N. and Robertson, A. (2005) Non-marine sedimentation associated with Oligocene–Recent exhumation and uplift of the Central Taurus, Mountains, S. Turkey. *Sedimentary Geology*, **173**, 53–89.

Kaçmaz, H. and Köktürk, U. (2004) Geochemistry and mineralogy of zeolitic tuffs from the Alaçatı (Çeşme) area, Turkey. *Clays and Clay Minerals*, **52**, 705–713.

Karakaş Z. and Kadir, S. (1998) Mineralogical and genetic relationships between carbonate and sepiolite-palygorskite formations in the Neogene lacustrine Konya Basin, Turkey. *Carbonates and Evaporites*, **13,** 198–206.

Khademi, H. and Mermut, A.R. (1998) Source of palygorskite in gypsiferous Aridisols and associated sediments from central Iran. *Clay Minerals*, **33**, 561–578.

Lang, J., Mahdoudi, M.L., and Pascal, A. (1990) Sedimentation-calcrete cycles in the Mesozoic Red formations from the central High atlas (Telouet area), Morocco. *Palaeogeography, Palaeoclimatology, Palaeoecology*, **81**, 9–93.

Moore, D.M. and Reynolds, R.C. (1989) *X-ray Diffraction and the Identification and Analysis of Clay Minerals*. Oxford University, Press, Oxford, UK, 332 pp.

Nazik, A. and Gökçen, N. (1989) Stratigraphical interpretation of the Ulukışla Tertiary sequences by ostracodes and foraminifers. *Geological Bulletin of Turkey*, **32**, 89–99 (in Turkish with English abstract).

Oktay, F.Y. (1982) Stratigraphy and geological history of Ulukısla and its surroundings. *Geological Bulletin of Turkey*, **25**, 15–23 (in Turkish with English abstract).

Rodas, M., Luque, F.J., Mas, R., and Garzon, M.G. (1994) Calcretes, palycretes and silcretes in the paleogene detrital sediments of the Dueo and Tajo Basins, central Spain. *Clay Minerals*, **29**, 273–285.

Rouchy, J.M. and Caruso, A. (2006) The Messinian salinity crisis in the Mediterranean basin: A reassessment of the data and an integrated scenario. *Sedimentary Geology*, **188**, 35–67.

Shadfan, H., Mashhady, A.S., Dixon, J.B., and Hussen, A.A. (1985) Palygorskite from Tertiary Formations of eastern Saudi Arabia. *Clays and Clay Minerals*, **33**, 451–457.

Singer, A. (1979) Palygorskite in sediments: Detrital, diagenetic or neoformed – A critical review. *International Journal of Earth Sciences*, **68**, 996–1008.

Singer, A. (1984) The palaeoclimatic interpretation of clay minerals in sediments – a review. *Earth-Science Reviews*, **21**, 251–293.

Torgersen T., De Decker P., Chivas, A.R., and Bowler J.M. (1986) Salt lakes; a discussion of processes influencing palaeoenvironmental interpretation and recommendation for future study. *Palaeogeography, Palaeoclimatology, Palaeoecology*, **54**, 7–19.

Verrecchia, E.P. and Le Coustumer, M.N. (1996) Occurrence and genesis of palygorskite and associated clay minerals in a pleistocene calcrete complex, Sde Boqer, Negev Desert, Israel. *Clay Minerals*, **31**,183–202.

Weaver, C.E. (1989) *Clays, Muds, and Shales*. Developments in Sedimentology, **44**, Elsevier, Amsterdam, 819 pp.

Weaver, C.E. and Beck, K.C. (1977) Miocene of the S.E. United States: a model for chemical sedimentation in a perimarine environment. *Sedimentary Geology*, **17**, 1–234.

Wedepohl, K.H. (1984) Die Zusammenzetzung der oberen Erdkruste und natürlicher Kreislauf ausgewalter Metalle. In *Metalle in der Unwelt* (E. Merian, editor). Verlag Chemie, Weinheim, Germany, 856 pp.

Yalçın, H. and Bozkaya, Ö. (2004) Ultramafic-rock-hosted vein sepiolite occurrences in the Ankara Ophiolitic Melange, Central Anatolia, Turkey. *Clays and Clay Minerals*, **52**, 227–239.

(*Received 7 April 2008; revised 29 August 2008; Ms. 0150; A.E. W. Huff*)